Assessing Impacts of Global Warming on Tropical Cyclone Tracks[*]

Liguang Wu

Goddard Earth and Technology Center, University of Maryland, Baltimore County, Baltimore, and Laboratory for Atmospheres, NASA Goddard Space Center, Greenbelt, Maryland

Bin Wang

Department of Meteorology, School of Ocean and Earth Science and Technology, University of Hawaii at Manoa, Honolulu, Hawaii

ABSTRACT

A new approach is proposed to assess the possible impacts of the global climate change on tropical cyclone (TC) tracks in the western North Pacific (WNP) basin. The idea is based on the premise that the future change of TC track characteristics is primarily determined by changes in large-scale environmental steering flows and in formation locations.

It is demonstrated that the main characteristics of the current climatology of TC tracks can be derived from the climatological mean velocity field of TC motion by using a trajectory model. The climatological mean velocity of TC motion, composed of the large-scale steering and beta drift, is determined on each grid of the basin. The mean large-scale steering flow is computed from the NCEP–NCAR reanalysis for the current climate state. The mean beta drift is estimated from the best-track data by removing the steering flow. The derived mean beta drift agrees well with the results of previous observational and numerical studies in terms of its direction and magnitude.

The approach is applied to assessing the potential impacts of global warming on TC tracks in the WNP. The possible changes in the large-scale steering flows are taken from the output wind fields of two Geophysical Fluid Dynamics Laboratory (GFDL) global warming experiments and possible changes in the TC formation locations are considered by shifting the formation locations as a whole. The GFDL experiments suggested that the changes in the future large-scale steering flows are dominated by the easterly anomalies in the Tropics and westerly anomalies in the midlatitudes with the enhanced northward component during the period of 2030–59. Based on the assessments using two different ways to reduce climate model biases, the prevailing TC tracks shift slightly southwestward during the period of 2000–29, but northeastward during the period of 2030–59. More TCs will take a recurving track and move northeastward during the period of 2030–59. The El Niño–like climate change predicted in many climate models can significantly enhance the track changes if the TC formation locations in the WNP shift eastward as a whole.

1. Introduction

The impacts of human activities on the global climate have been of great concern since the last century. Scientific research has indicated that human activities are changing atmospheric composition in ways that are very likely to cause significant global warming. The United Nations' Intergovernmental Panel on Climate Change (IPCC) has speculated that climate change due to increasing amounts of anthropogenic greenhouse gases may affect tropical sea surface temperature (Houghton

et al. 1996), and thus tropical cyclone (TC) intensity (Knutson and Tuleya 2001; Walsh and Ryan 2000).

By now we know little about the possible impacts of the climate change on TC tracks. Assessment of the global warming impacts on TC activity remains in question. Manabe et al. (1970) noticed for the first time that atmospheric general circulation models (AGCMs) are able to simulate model tropical storms that have a climatology and physical characteristics similar to those of real tropical storms. Studies have been conducted to investigate the variability of TC formation on various time scales in AGCMs (e.g., Broccoli and Manabe 1990; Wu and Lau 1992; Haarsma et al. 1993; Bengtsson et al. 1996; Vitart and Anderson 2001). According to Henderson-Sellers et al. (1998), however, current AGCMs cannot adequately simulate TCs to the degree that one can possibly say whether the frequency, area of occurrence, time of occurrence, mean intensity or maximum intensity of TCs would change in the global warming

Corresponding author address: Dr. Liguang Wu, NASA GSFC, Code 912, Greenbelt, MD 20771.
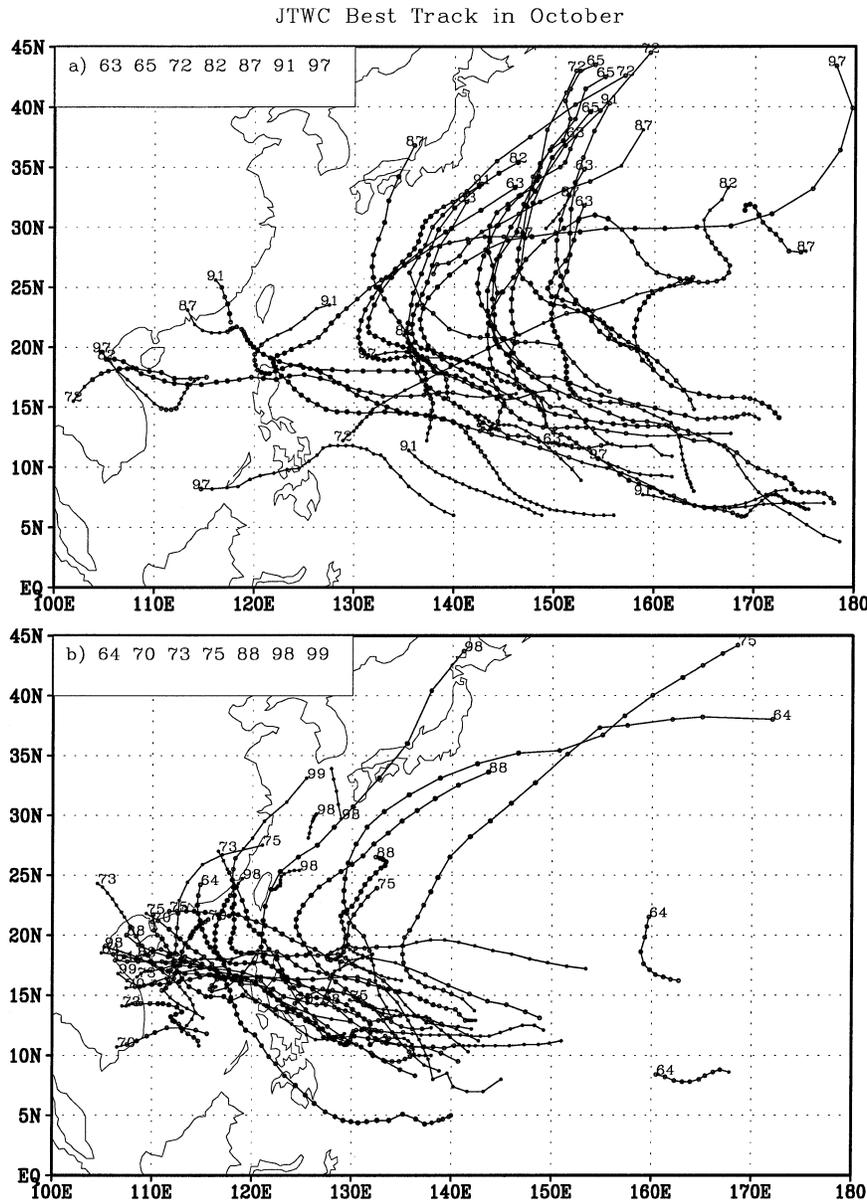E-mail: liguang@agnes.gsfc.nasa.gov

JTWC Best Track in October

FIG. 1. The TC tracks in Oct of (a) El Niño years (1963, 1965, 1972, 1982, 1987, 1991, 1997) and (b) La Niña years (1964, 1970, 1973, 1975, 1988, 1998, 1999).

scenario. Considering that the large-scale atmospheric circulation simulated in GCMs may be more reliable than the model-simulated so-called TCs, Watterson et al. (1995) calculated the indices for TC formation developed by Gray (1975) in an AGCM in an attempt to indirectly estimate TC formation numbers. So far, little attention has been paid to the possible future changes in TC tracks.

The prevailing TC track is intimately linked to the mean large-scale circulation patterns. Recently, Wang and Chan (2002) examined how El Niño–La Niña affect the TC activity over the western North Pacific. They found that during October of El Niño years tropical storms tend to recurve northward to the extratropics, whereas during the October of La Niña years tropical storms more frequently take a westward track (Fig. 1). In addition, the formation locations shifted eastward dramatically in El Niño years. The changes in the large-scale steering flows induced by El Niño forcing are evident (Fig. 2). The increased number of the northward-turning tropical storms near Japan during El Niño years is consistent with the increased northward steering flows (vertically averaged between 850 and 300 hPa) (Fig. 2b). The decrease in the number of westward-moving tropical storms from the Philippine Sea to the southeast Chinese coast during El Niño years is also in
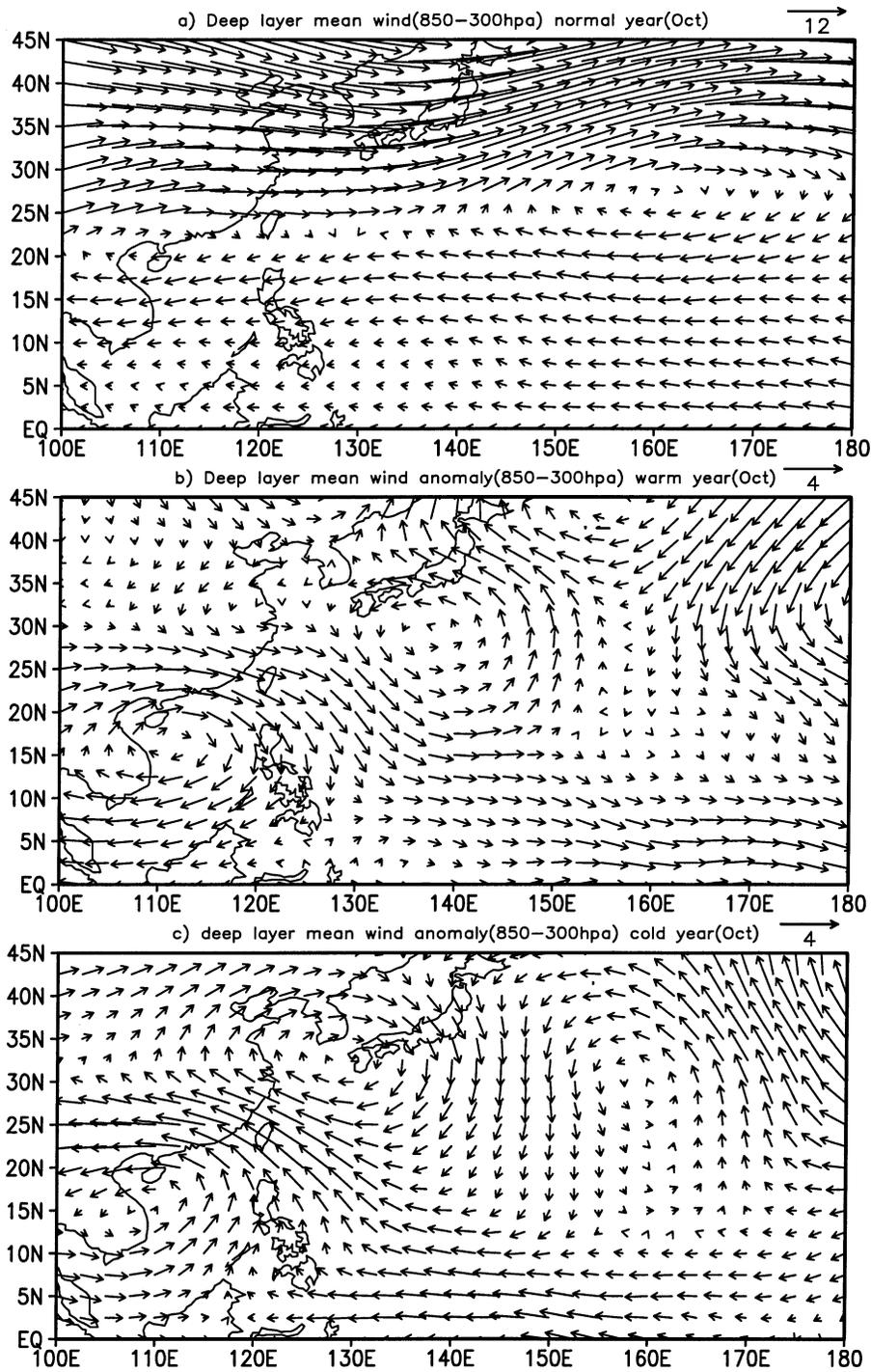
FIG. 2. Oct climatological layer (850-300 mb) mean flows for (a) normal years, and layer wind anomalies for (b) El Niño warm years (1963, 1965, 1972, 1982, 1987, 1991, 1997) and (c) La Niña cold years (1964, 1970, 1973, 1975, 1988, 1998, and 1999).

good agreement with the decrease of the easterly steering currents in the region (Fig. 2b). It is inferred that during global warming background changes in the large-scale flow pattern and the TC formation locations may effectively change the tropical storm track and their impacts to human life.

Recent progress in TC motion research has made it more meaningful to assess the future changes of TC

tracks based on projected future changes in the general circulation. It is now generally recognized that two fundamental mechanisms operating in TC motion are (i) advection of the relative vorticity or potential vorticity associated with the TC by large-scale environmental flows (large-scale steering) and (ii) propagation or beta drift that involves the nonlinear interactions among the environmental flow, the planetary vorticity gradient, and the vortex circulation (Wang et al. 1998). Numerical and observational studies suggest that the propagation component can be 2–4 m s^{-1} and it becomes important in causing a systematic deviation when the steering currents are weak (Wang and Li 1992; Wang and Holland 1996; Carr and Elsberry 1990; Franklin et al. 1996).

The insights gained from the TC motion research provide a basis for evaluation of the global warming impacts on TC tracks. In order to relate the climatology of TC tracks to the global climate change, we propose to define mean storm motion as the sum of the climatological mean large-scale steering flow and beta drift. The mean motion is indicated by the climatological mean velocity of TC motion on specified grids. It is hypothesized that the mean velocity defined on specified grids can be used to derive the primary features of the climatological mean TC tracks. It is conceivable that the climatology of TC tracks may respond to the global climate change due to the resultant changes in large-scale steering flows.

Compared with the climate change, TCs are short-lived and transient phenomena. For a specific TC, it is extremely difficult to separate the environmental steering from the TC circulation. Many earlier efforts were mainly concentrated on searching for the steering flow from various observations. On the time scale of climate change, however, this problem is not relevant because the transient TCs have been substantially removed from the climatological mean environmental flows. Recently, Wu and Wang (2001) have verified that there exits a steering level for a specific TC in the diabatic numerical experiments. Although such a steering level varies case by case, they showed that the steering level is located in the lower and middle troposphere. As suggested by Holland (1993), the pressure-weighted mean flow from 850 to 300 mb will be taken as the steering flow.

In this study, an approach for assessing the impacts of climate change on TC tracks is proposed. Using this approach, the future changes of TC track are evaluated with the output of the global warming experiments of the Geophysical Fluid Dynamics Laboratory (GFDL) rhomboidal 30 truncation (R30) coupled climate model (Delworth et al. 2002). Our focus is placed on the western North Pacific (WNP). The WNP basin experiences on average 26 tropical cyclones each year, accounting for about 33% of the global total. In east Asia, vulnerability becomes more and more pronounced due to recent fast population growth and economic development in the coastal region. Any possible climatological shift of TC tracks is of great importance to both the govern-

ments and the public. In particular, two questions will be addressed: 1) Will the typical cyclone tracks shift due to the climate change? 2) How will the primary pattern of the WNP TC track change in response to the global climate change?

The paper is therefore organized as follows. Section 2 defines three parameters that measure the climatological characteristics of TC tracks. Section 3 shows how climatological characteristics of TC tracks can be derived from climatological mean velocity by using a trajectory model. In section 4 the climatological mean beta drift is retrieved and compared with results from the previous studies. The future climatological TC motion is estimated in section 5. Section 6 discusses to what extent the global climate change can modify the TC tracks. Concluding remarks are presented in section 7.

2. Climatology of TC motion in the western North Pacific

The climatological TC motion can be measured by the following three parameters: 1) the distribution of the frequency of TC occurrence within a TC basin; 2) the frequency of TCs that enter a larger region within a TC basin; and 3) climatological mean velocity of TC motion.

The first is defined on each grid box to indicate the spatial distribution of TC activities. It is counted at a 6-h interval and measures how frequently a specific grid box is affected by storms. The grid box is 2.5° latitude by 2.5° longitude in this study. Figures 3a and 4 show, respectively, the frequency of occurrence and the formation frequency in each grid box during July–September calculated using the Joint Typhoon Warning Center (JTWC) best-track data (BTD) from 1965 to 2000. The starting year was chosen to be 1965 when satellite monitoring of weather events first became routine so that no TC would be missed. During the peak season from July to September, there are two maximum centers for TC occurrence, which are located to the east of Taiwan and the South China Sea, respectively. Although a maximum of the formation frequency (Fig. 4) coincides with the center in the South China Sea, the formation frequency only accounts for a very small fraction of the total frequency of TC occurrence. In other words, the distribution of TC frequency within the WNP basin is primarily a reflection of TC motion.

The second parameter measures how many TCs hit a specific region of interest. In general, a TC that forms over the WNP takes one of the three typical tracks: westward, northwestward, and northeastward recurving. Accordingly, it would affect the following regions: the South China Sea region (including Philippines), the coastal region of China (including the Taiwan island), and the Japan region (Fig. 5). What we want to know is whether the typical tracks change in response to the global climate change. The percentage is calculated based on the total storms of the three categories. During
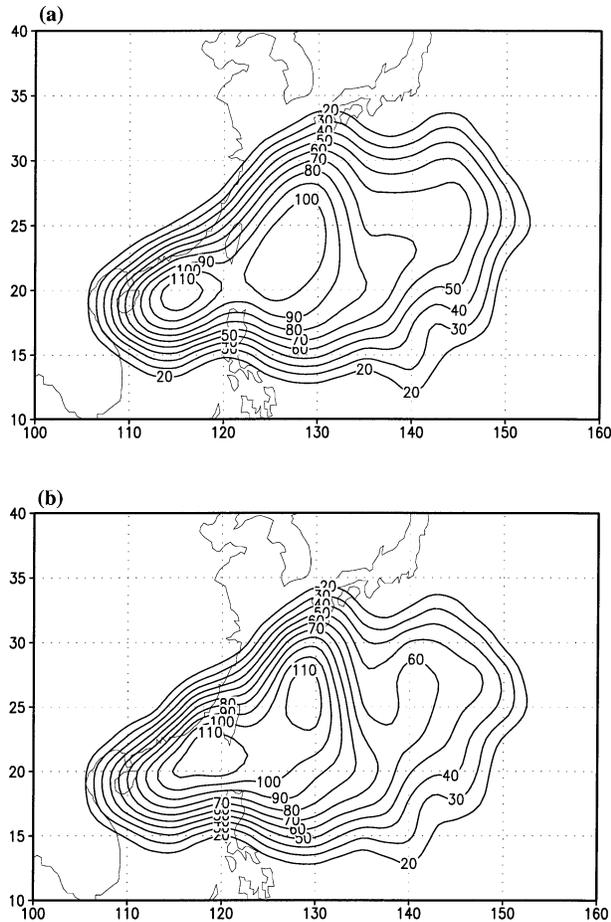
(a)

(b)

FIG. 3. Distribution of the frequency of TC occurrence at 2.5° × 2.5° resolution in the typhoon peak season (Jul–Sep) derived from (a) the JTWC best-track data from 1965 to 2000 and (b) the trajectory model.
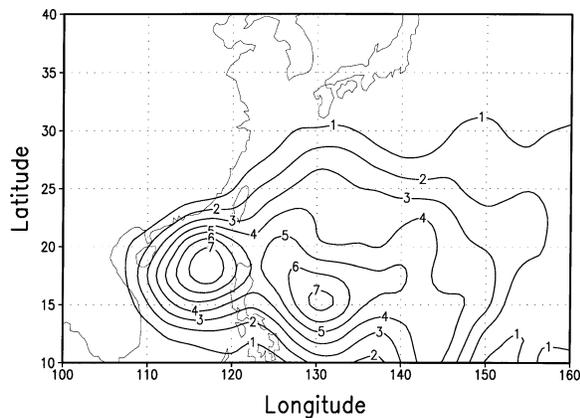

FIG. 4. Distribution of the TC formation frequency at each 2.5° × 2.5° grid point in the typhoon peak season (Jul–Sep) derived from the JTWC best-track data from 1965 to 2000.
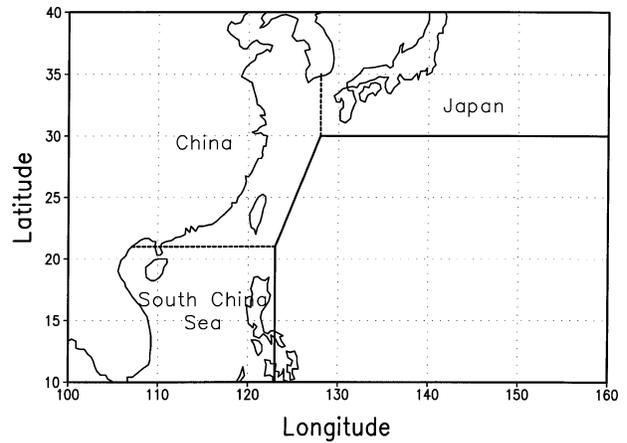

FIG. 5. Schematic of the regions where the possible impacts of the global climate change on TC tracks are investigated. The three regions are the South China Sea, the eastern coastal region of China, and the Japan region.

the period of July–September, based on the best-track data from 1965 to 2000, 14.1%, 37.9%, and 47.9% of the storms affect those three regions, respectively (Table 1). It should be pointed out that a storm may be counted twice if it entered the South China Sea and then moved northward to enter the east coastal region of China.

The third parameter is also defined on each grid box. As done by Carr and Elsberry (1990), the TC motion is transferred into a fixed reference frame relative to the earth. The mean velocity of TC motion is calculated at each grid point based on all the storms that passed across a grid point. In the present study, a grid point represents a box of 2.5° latitude by 2.5° longitude. Figure 6 shows the mean TC translation vectors. Note that the mean translation vector is consistent with the seasonal mean steering flows. During the peak season (July–September), TCs occur frequently and the large-scale flows are relatively steady. In this case, the climatological mean flows can be taken as the climatological steering flows. In other months, the climatological mean flows may not be a good indicator for the mean large-scale steering flows because TCs may not occur frequently enough to render a statistically reliable mean motion vector, or because the large-scale flows are unsteady. The choice of the period of July–September is based on such consideration.

3. The trajectory model

In this section, we demonstrate that the climatological features of the TC tracks can be deduced from clima-

TABLE 1. Comparisons of the trajectory model-derived percentage of TCs affecting the three regions with observations.

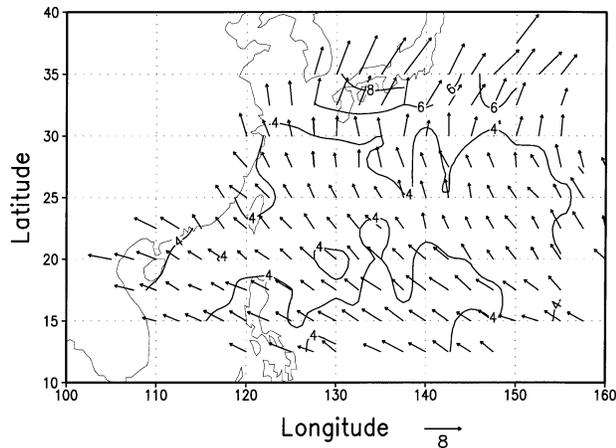|	South China Sea	China	Japan
BTD	14.1	37.9	47.9
SIM	14.6	37.9	47.3
CTRL	1.6	47.4	51.0

FIG. 6. Mean TC translation vectors and magnitudes (m s^{-1}, contours) in the typhoon peak season derived from the JTWC best-track data from 1965 to 2000. Contour interval is 2 m s^{-1}.

tological mean motion vectors by using a trajectory model. In this model, a TC is treated as a point vortex, and moves with the climatological mean translation velocity within a specified grid box. In other words, all the storms located within the same grid box move at the same speed. To construct the climatology of TC tracks from the the climatological mean translation velocity, all the tropical storms that formed during the peak season of 1965–2000 are considered. The initial position of a storm is its location when it first achieved its tropical storm intensity. The trajectory calculations end when the storms move out of the whole domain. For the grids on which the climatological motion vectors are not available, the velocity is taken as the sum of the mean steering flow and the mean beta drift that was computed by averaging the beta drift over all the grids on which the climatological motion vectors are available. The TC trajectories from 1965 to 2000 can be simulated with the climatological mean TC motion vectors derived in section 2. For convenience, this is called experiment SIM. With the simulated TC trajectories, the frequency of TC occurrence can be derived as discussed in section 2. Figure 3b shows the simulated frequency of TC occurrence. It is nearly identical to Fig. 3a. The magnitude near the major center is slightly overestimated. It should be noted that the calculated trajectories are meaningful within the domain encircled by the contour of 40 since we assume that a reasonable estimate of the climatological motion vectors may not be available beyond the domain.

With the simulated trajectories, the numbers of TCs that affect the three regions mentioned earlier can be deduced. During the peak season, based on the simulated trajectories (SIM), 14.6%, 37.9%, and 47.3% of the storms, affect the South China Sea, the coastal region of China, and the Japan region, respectively (Table 1). The differences of the percentage of TCs affecting the three typical regions between SIM and the best track

data are within 1% of the error bars. It is shown that the first two parameters that indicate the climatological characteristics of TC tracks in the WNP can be well retrieved from the climatological mean velocity, and that the trajectory model provides a way to assess the response of TC tracks to the global climate change if the climatological motion velocities can be estimated from climate models.

4. Retrieval of climatological beta drift

The propagation component of TCs has been extensively studied with barotropic and baroclinic numerical models. Due to the beta effect, even in a resting environment a TC would move northwestward in the Northern Hemisphere (Adem 1956; Holland 1983). In a three-layer model, Shapiro (1992) found that the beta drift is about 2.4 m s^{-1} toward the north-northwest. Recently numerical studies (Wang and Holland 1996; Wu and Wang 2001) confirmed this finding. Although the influence of environmental flows varied in different models, especially for the vertical shears of the environmental flow, it is generally believed that beta drift can be affected by the large-scale environmental flow (Williams and Chan 1994; Wang and Li 1995; Li and Wang 1996; Shapiro 1992; Flatau et al. 1994; Wang and Holland 1996; Wu and Wang 2001).

Despite uncertainties involved in defining a large-scale steering flow, a persistent difference between the steering flow and the TC motion is found to be northwestward in the Northern Hemisphere (George and Gray 1976). Carr and Elsberry (1990) converted the composite rawinsonde studies to a north-oriented, earth-relative coordinate system and displayed the difference vectors between cyclone motion and the layer-mean (850–300 hPa) steering flow averaged over a 5°–7° latitude band of the TC center. In agreement with the numerical studies, they found that the beta drift or propagation is generally westward and poleward in each hemisphere with magnitudes ranging from 1–3 m s^{-1}. Franklin (1990) analyzed the case of Hurricane Josephine and found that the difference ranges from 1.8–3.7 m s^{-1} with the directions from 289°–317°. Franklin et al. (1996) used Omega dropwindsonde datasets for 10 Atlantic TCs and showed that the propagation vector has the mean orientation of 321° and mean magnitude of 3.2 m s^{-1}.

Following Holland (1993), a single large-scale steering flow is defined in this study as the pressure-weighted mean flow from 850 to 300 hPa (see also Carr and Elsberry 1990). The climatological wind data from the National Centers for Environmental Prediction–National Center for Atmospheric Research (NCEP–NCAR) reanalysis are based on 13-yr average monthly fields from 1982 to 1994 with a uniform latitude–longitude 2.5° resolution. As mentioned earlier, the climatological mean propagation component can be obtained by removing the climatological mean steering flow from the
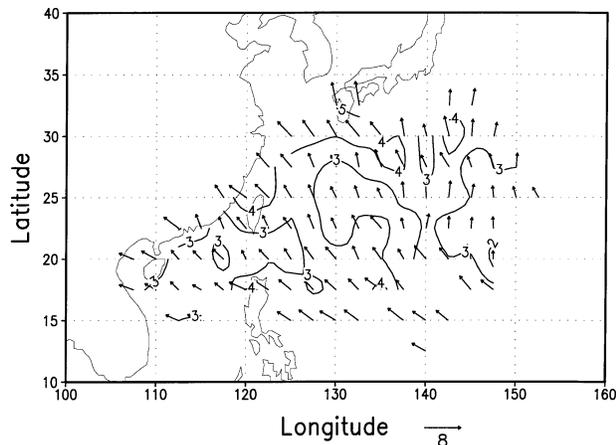
FIG. 7. Mean propagation vectors and magnitudes (m s^{-1}, contours) in the typhoon peak season derived from the JTWC best-track data from 1965 to 2000. Contour interval is 1 m s^{-1}. Each grid point has at least 40 samples.
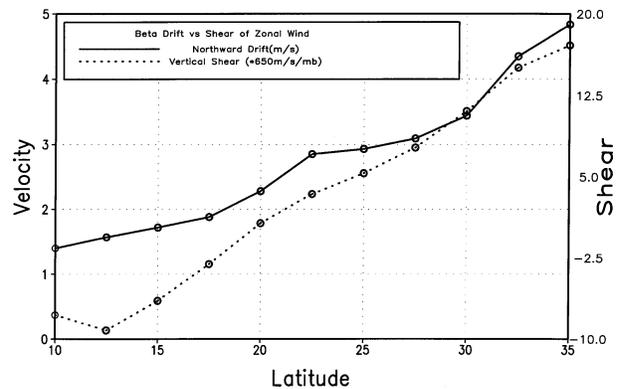

FIG. 8. Northward beta drift velocity and vertical shear of the zonal mean environmental flows as a function of latitude. The vertical shear is defined as the wind difference between 200 and 850 mb.

climatological mean translation vectors shown in Fig. 6. As shown in Fig. 7, the resulting mean beta drift is generally westward and northward, which is consistent with the previous observational studies (Carr and Elsberry 1990; Franklin et al. 1996) and numerical studies (Wang and Li 1992; Wang and Holland 1996). There are several vectors near the center of the subtropical high that are eastward. This may be because the climatological steering flow is not well represented by the climatological mean flow. As we know, TCs usually cannot move into the center of the subtropical high. The mean orientation of the beta drift is 303° with a mean magnitude of 3.0 m s^{-1}. This compares well with the 321° direction of the beta drift with a mean magnitude of 3.2 m s^{-1} found in Omega dropwindsonde datasets (Franklin et al. 1996). It is larger than the magnitude of 1–2.5 m s^{-1} from composite analysis (Carr and Elsberry 1990).

Chan and Williams (1987) and Wang and Li (1992) suggested that the beta drift was proportional to the gradient of the Coriolis parameter. The mean propagation components are averaged by latitudes to examine the latitudinal dependence. In the presence of environmental flow, the observed results differ from the numerical model studies; the northward component increases with latitudes (Fig. 8). This agrees with Carr and Elsberry's finding that the beta drift direction rotates from northwestward to north-northwestward with latitudes. We find that the increase is accompanied by the increase of the vertical shear of the zonal environmental flow. According to Wu and Emanuel (1993), Flatau et al. (1994), and Jones (1995), the vertical shear can significantly tilt a TC and then enhance the northward propagation. Wang and Holland (1996) suggest that the enhanced northward drift arises from the penetration flow of the upper-level anticyclone associated with TCs. Wu and Wang (2001) suggested that the resulting asym-

metric circulation is responsible for the enhanced northward drift. Therefore the latitude-dependence may reflect the influence of the vertical shear of environmental flows. Furthermore, the meridional shear of the environmental flow—in particular, the shear strain rate—can significantly change the beta drift (Wang and Li 1995; Li and Wang 1996; Wang et al. 1997).

In this section, the climatological mean beta drift has been derived from the best-track data by subtracting the steering flow from the actual storm motion. The derived beta drift agrees well with the previous numerical and observational studies in terms of its magnitude and direction. In addition, the influence of the vertical environmental shears on beta drift is also shown, which has been confirmed through various numerical model studies. These results suggest that the selected large-scale steering flow is reasonable.

5. Estimating future climatological TC motion

In section 3, it was demonstrated that the main climatological characteristics of TC tracks can be deduced from the climatological mean motion vectors. In order to obtain the future climatological features of TC tracks, the new climatological mean motion vectors in the projected future climate state must be constructed. The construction of the future mean beta drift remains a challenge. Up to now it has been found that the beta drift can be affected by the strength of TCs, the vertical and horizontal shears of the environmental flows, and the relative vorticity gradient of the environmental flow. To simplify the analysis, it is assumed that the global climate change would only significantly modify the large-scale environmental flow on the zero order. The changes on the first order (horizontal and vertical shears) and on the second order (relative vorticity gradients) are neglected. The beta drift is assumed not to change from the present-day climate.

The large-scale steering flow in the projected future climate state is calculated from the output wind fields
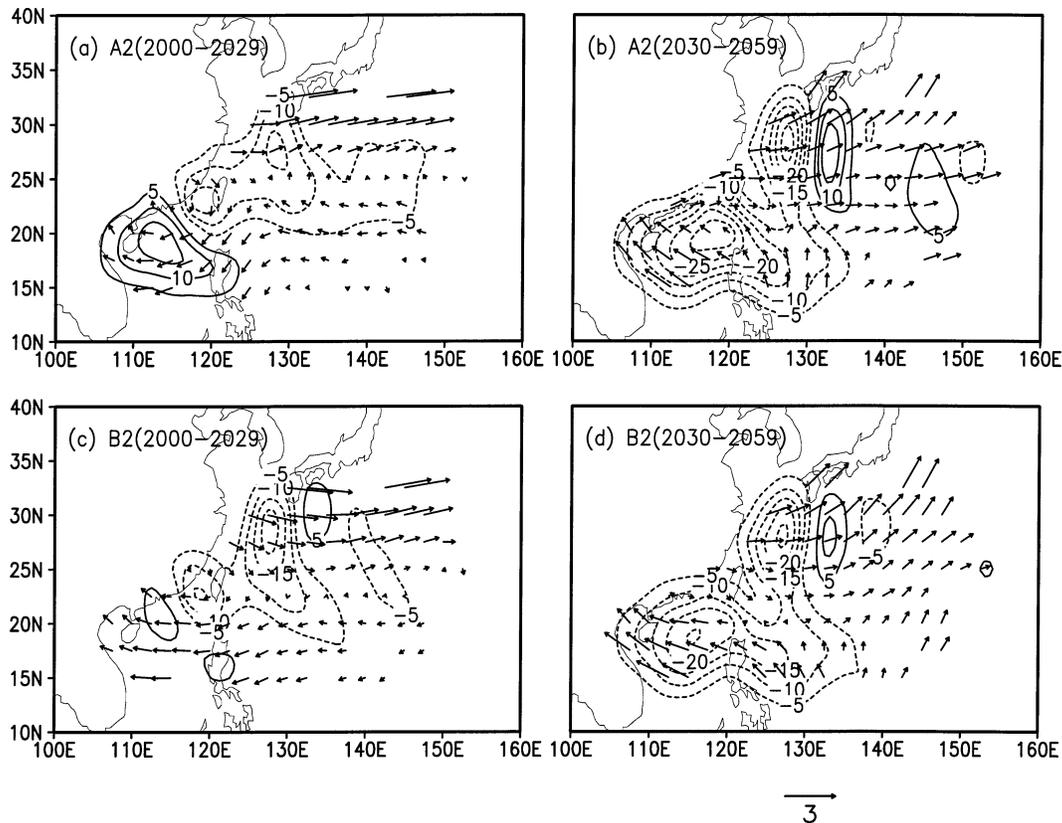
Fig. 9. Simulated deviations of large-scale steering flows (m s^{-1}) calculated with the first approach from the current climate state in the GFDL global warming experiments and the derived changes in the frequency of TC occurrence for the peak season of Jul–Sep: experiments (a) A2 for 2000–29; (b) A2 for 2030–59; (c) B2 for 2000–29; and (d) B2 for 2030–2059.

of two global warming experiments using the GFDL climate model with IPCC scenario forcing A2 and B2 (Delworth et al. 2002). The data were downloaded from the Internet at nomads.gfdl.noaa.gov. The atmospheric component of the coupled model uses a spectral technique with rhomboidal 30 truncation, which corresponds to a transform grid with a resolution of approximately 2.25° latitude by 3.75° longitude. The ocean component has a resolution of approximately 2.25° latitude by 1.875° longitude. Relatively simple formulations of river routing, sea ice, and land surface processes are included (Delworth et al. 2002).

The main difference between these two experiments is the level of the global CO_2 emission. In experiment A2, global CO_2 emission can increase by more than fourfold over their 1990 level by 2100 because it is

TABLE 2. Differences of the percentage of TCs affecting the three regions using the first approach to reduce the climate model biases.

		South China Sea	China	Japan
2000–29	A2	4.2	−2.4	−1.2
	B2	3.2	−1.7	−1.4
2030–59	A2	−4.8	−6.2	11.1
	B2	−2.8	−6.9	7.8

assumed that fossil fuels maintain their dominant roles in the energy supply. On the other hand, in experiment B2, global CO_2 emission increases relatively slowly. With the continued growth of population and of income per capita, the level of global CO_2 emissions increases about twice the 1990 level by 2100 (Houghton et al. 2001). As shown in the IPCC 2001 report, although the CO_2 emission in the scenario A2 is significantly higher than that in B2, the difference in simulated global-mean temperature is small between the two scenarios. The A2 temperature is slightly lower than the B2 temperature in the first half of the twenty-first century, probably due to a difference in SO_2 emissions.

As we know, large uncertainties exist in climate model prediction. Some uncertainties can result from model biases. As a result, the simulated current climate state can be different from the observations. In order to reduce the influence of the model biases, the output data from the GFDL R30 control experiment (ctrl_06) are used. An additional experiment is performed as experiment SIM, but the large-scale steering flow was calculated from the output of experiment ctrl_06. For convenience, this experiment is called CTRL. In Table 1, the percentage of the TCs affecting the three typical
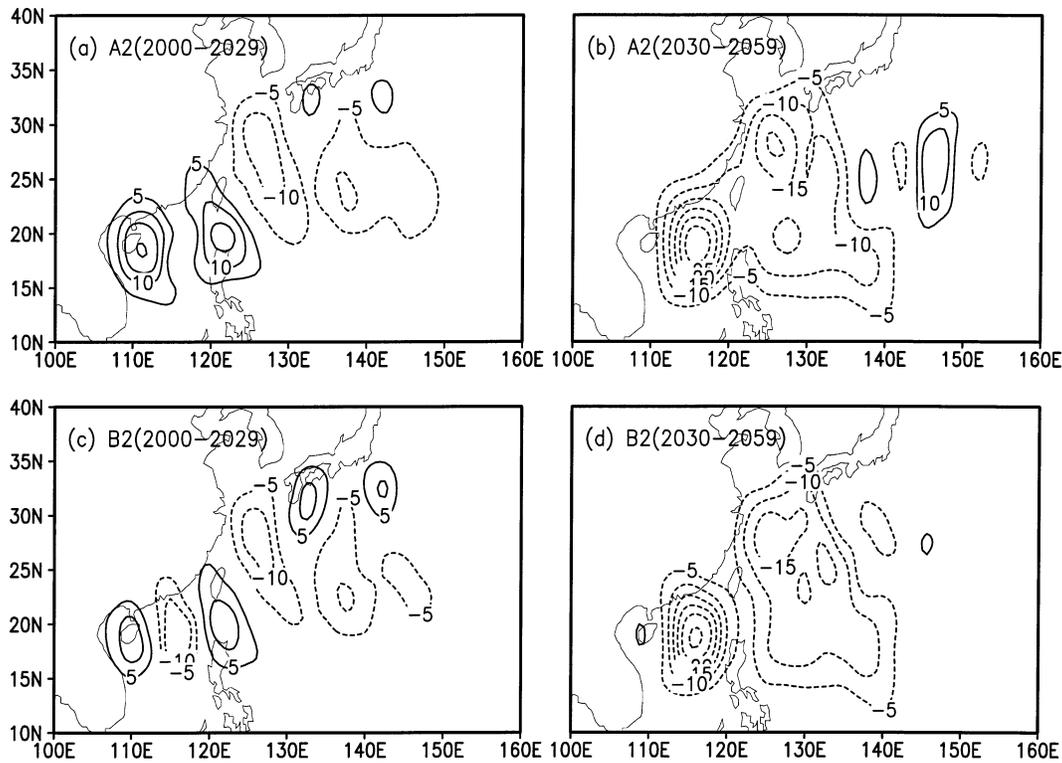
FIG. 10. Same as in Fig. 9 but only for the derived changes in the frequency of TC occurrence using the second approach.

regions based on this experiment is also shown (the third row). Comparisons of the results with those in experiment SIM and BTD indicate that there are significant biases in the simulated current climate state.

In principle, two approaches can be used to derive the potential impacts of global climate change on TC tracks in terms of finding the way to reduce model biases. First, the changes of large-scale steering flow caused by the global warming are considered; these are the deviations of the projected steering flows in A2 and B2 from those in the GFDL control experiment (experiment ctrl_06). The future climatological mean steering flows are the sum of these anomalies and the climatological mean steering flows in the current climate state. The simulated TC trajectories can directly be compared with those in experiment SIM. Second, the future large-scale steering flow was calculated directly from the projected wind fields in experiments A2 and B2. Of course, the derived TC trajectories include the influence

of the model biases. In this case, the model biases can be removed by comparing the frequencies of TC occurrence in a specified region and in a specific location with those in experiment CTRL. The results using these two approaches will be addressed in the next section.

6. Potential impacts of global climate change on TC tracks

The potential impacts of global warming on TC tracks are first assessed by examining the influence of changes in the large-scale steering flow for the periods of 2000–29 and 2030–59. Figure 9 shows the distribution of the deviations of the mean TC motion vectors or the large-scale steering flows in GFDL experiments A2 and B2 from those in the current climate state and the corresponding changes in the frequency of TC occurrence. The anomaly patterns are similar in both experiments, which are dominated by the easterly anomalies in the Tropics and westerly anomalies in the midlatitudes. Careful examination indicates that changes in the steering flow will occur from 2000–29 to 2030–59. During the second period (2030–59), the northward component will be enhanced almost in the whole basin. In particular, the anomalies over the TC formation region east of 130°E and south of 25°N will change from the weak easterly to the southwesterly.

In order to demonstrate the implications of these de-

TABLE 3. Same as in Table 2 but using the second approach to reduce the climate model biases.

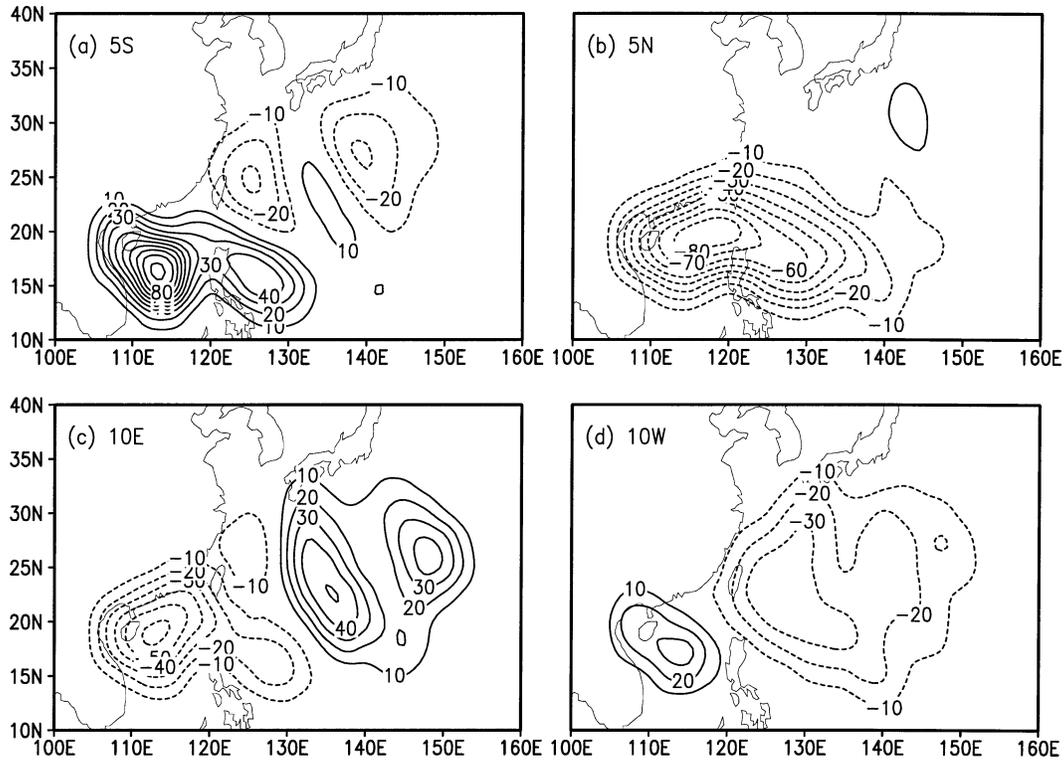|		South China Sea	China	Japan
2000–29	A2	3.1	−4.2	1.3
	B2	3.0	−3.3	0.3
2030–59	A2	−0.6	−10.6	11.1
	B2	0.5	−9.5	9.0

FIG. 11. Sensitivity of the frequency of TC occurrence to the shifts of TC formation locations: (a) 5° southward, (b) 5° northward, (c) 10° eastward, and (d) 10° westward.

viations of large-scale steering flows, the trajectories of TCs are calculated based upon the frequency and position of TCs formed during 1965–2000. Here the future TC motion vectors were constructed using the first approach discussed in section 5. Two primary centers of TC activities are located roughly in the same location as in Fig. 3 (figures not shown), indicating no significant changes in the TC activity centers under both IPCC scenarios A2 and B2. During the period of 2000–29, the frequency of TC occurrence over the ocean between Japan and the Philippine Sea will decrease, but increases over the South China Sea (Fig. 9), suggesting a slightly southwestward shift of the typical TC tracks during the period of 2000–29 due to the enhanced easterly component of steering flows in the low latitudes. The number of TCs affecting the South China Sea region increases by 4.2% in A2 and 3.2% in B2, while the numbers of TCs affecting the regions of China and Japan experience a slight decrease (Table 2).

During the second period (2030–59), the changes are generally more significant than those in the first period as the IPCC scenario forcing becomes stronger. The western part of the basin including the South China Sea, the Philippine Sea, and the East China Sea experiences significant reduction in the frequency of TC occurrence and small increase can be seen in the eastern part of the basin (Fig. 9). A possible reason is that the enhanced northward component of the wind anomalies south of

Japan let more TCs recurve before they enter the South China Sea region. The regions of the South China Sea and China will experience less TCs during this period. The decrease ranges from 2.8% in B2 to 4.8% in A2 for the South China Sea and from 6.2% in A2 to 6.9% in B2 for the region of China. On the other hand, the TC number affecting the region of Japan increases by 11.1% in A2 and 7.8% in B2. Although the northeastward anomalies extending from the low latitudes to the region south of Japan indicate that TCs have more chance to recurve and move northeastward, the increase of the frequency of TC occurrence in the eastern part of the domain is not significant because the frequency of TC occurrence is also determined by the TC speed (Figs. 9b,d).

The influence of global warming on the frequency of TC occurrence was also assessed using the second approach discussed in section 5. Comparing the changes of the frequency of TC occurrence in Fig. 10 with those in Fig. 9 indicates that both approaches give very similar assessments. Comparing Table 2 with Table 3 indicates that both approaches predict small changes in the Japan region during the period of 2000–29. The second approach also predicts very small changes in the South China Sea region during the period of 2030–59, suggesting that the increase of TC occurrence over Japan during this period arises mainly from the decrease of
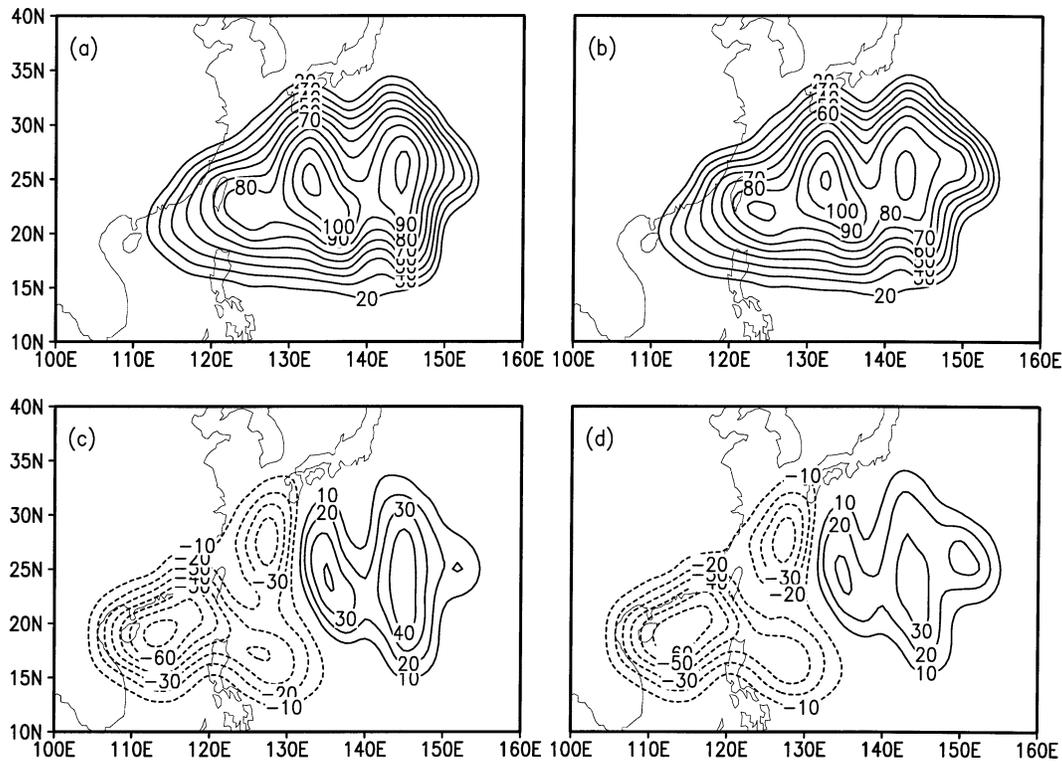
FIG. 12. Frequency of TC occurrence for GFDL experiments (a) A2 and (b) B2 and its deviations from the current climate state using the first approach for (c) A2 and (d) B2 during the period of 2030–59 with the TC formation location shifted eastward by 10°.

TC occurrence over East China Sea region, not from the South China Sea region.

In the earlier discussion, shifts in the TC formation locations were ignored. However, as suggested in Fig. 1, these locations can shift as a whole. In order to examine the sensitivity of TC tracks to the possible shifts, four experiments are performed to shift all the locations of TC formation from 1965 to 2000 5° southward (5S), 5° northward (5N), 10° eastward (10E), and 10° westward (10W), respectively. Note that the observed TC motion vectors in the current climate state are used in these experiments. Figure 11 indicates that more significant changes in TC tracks can occur if the formation locations shift as a whole. The frequency of TC occurrence over the Philippine Sea and the South China Sea will significantly increase (decrease) if the formation locations shift 5° southward (northward). The region south of Japan experiences more (less) TCs, and the South China Sea experiences less (more) TCs if the formation locations shift 10° eastward (westward). It is suggested that the shift of formation locations can have larger influence on tracks than the projected changes in large-scale steering flows.

Recent climate model studies suggested that the trends for surface temperature become more El Niño–like in the tropical Pacific, with the eastern tropical Pacific warming more than the western tropical Pacific,

with a corresponding eastern shift of precipitation (Houghton et al. 2001). In this sense, it is possible for the TC formation locations to shift eastward in response to these large-scale circulation changes. The experiment 10E was conducted again with the projected anomalies of the large-scale steering flow in the GFDL global warming experiments. Figure 12 shows the possible impacts on TC tracks in response to the changes both in steering flows and the shifted formation location during the period of 2030–59. Comparisons of Figs. 12a and 12b with Figs. 3a and 3b indicate that the prevailing TC tracks will dramatically shift eastward. A new center of TC activity is located in the eastern part of the basin, whereas the frequencies of TCs that affect the South China Sea, the Philippine Sea, and the East China Sea are significantly reduced (Figs. 12c,d). In other words, more TCs in the WNP basin will take a northeastern recurving track.

7. Summary

An attempt is made to assess the possible impacts of the global climate change on TC tracks in the WNP. A climatological mean vector of TC motion on each grid point is first determined, based on all storms that passed across the grid point. The primary climatological features, such as the frequency of TC occurrence in a spe-

cific location and the frequency of TCs that enter a specified landfalling region or extratropics, can be derived from the climatological mean motion vector field. In order to assess the impacts of climate change on TC tracks, the mean motion vector in the future climate state is computed as to the sum of the future climatological mean large-scale steering flow and the mean beta drift. The mean beta drift was determined from current climatology and assumed unchanged. In other words, the influence of the global climate change on TC tracks are investigated by examining how the climate change alters the climatological mean steering flow and TC formation locations.

The climatological mean beta drift was estimated from the best-track data. The resulting beta drift is in good agreement with the previous numerical and observational studies in terms of the magnitudes and directions. It is also found that the vertical shears can have significant influence on the beta drift. The results agree with numerical studies (e.g., Wu and Emanuel 1993; Jones 1995).

The potential impacts of global warming on TC tracks in the WNP are assessed by including the possible changes both in the large-scale steering flows, which are calculated from the output wind fields of GFDL global warming experiments A2 and B2, and in the formation locations. The GFDL R30 model projected that the changes in large-scale steering flows are dominated by the easterly anomalies in the Tropics and westerly anomalies in the midlatitudes with the enhanced northward component during the period of 2030–59. Accordingly, the typical TC tracks slightly shift southward during the period of 2000–29, northeastward during the period of 2030–59. The WNP basin can experience more northeastern recurving TCs during years 2030–59. The possible shifts in TC formation locations are also examined by shifting the formation locations as a whole. It is suggested that the shift of TC formation locations can have larger influence on TC tracks than the projected changes in large-scale steering flows. If the TC formation locations shift eastward as a whole due to the El Niño–like climate change predicted in many climate models, the northeastward shift in TC tracks in the WNP can be significantly enhanced during the period of 2030–59.

It should be pointed out that the main objective of this study is to propose a new approach to assess the potential impacts of global warming on TC tracks. The GFDL climate model outputs are used to illustrate the implications of this approach. The results should be interpreted in combination with the following assumptions made in this study. First, since the results are derived from the output of the GFDL climate model, the results are strongly affected by the accuracy of the model prediction. Second, the response of the mean beta drift on the global climate change is not considered. Third, the total TC number has been assumed to be the same as in the current climate state. As mentioned in section 4,

the mean beta drift could be affected by the large-scale environmental flow through the vertical and horizontal shears, shear strains, and vorticity gradients. Future study will include the outputs of different climate models and evaluate the model capabilities to simulate the large-scale circulation.

REFERENCES

Adem, J., 1956: A series solution for the barotropic vorticity equation and its application in the study of atmospheric vortices. *Tellus,* **8,** 364–372.

Bengtsson, L., M. Botzet, and M. Esch, 1996: Will greenhouse gas induced warming over the next 50 years lead to higher frequency and greater intensity of hurricanes? *Tellus,* **48A,** 57–73.

Broccoli, A. J., and S. Manabe, 1990: Can existing climate models be used to study anthropogenic changes in tropical cyclones climate? *Geophys. Res. Lett.,* **17,** 1917–1920.

Carr, L. E., and R. L. Elsberry, 1990: Observational evidence for predictions of tropical cyclone propagation relative to steering. *J. Atmos. Sci.,* **47,** 542–546.

Chan, J. C.-L., and R. T. Williams, 1987: Analytical and numerical studies of beta-effect in tropical cyclone motion. Part I: Zero mean flow. *J. Atmos. Sci.,* **44,** 1257–1265.

Delworth, T. L., R. J. Stouffer, K. W. Dixon, M. J. Spelman, T. R. Knutson, A. J. Broccoli, P. J. Kushner, and R. T. Wetherald, 2002: Review of simulations of climate variability and change with the GFDL R30 coupled climate model. *Climate Dyn.,* **19,** 555–574.

Flatau, M., W. H. Schubert, and D. E. Stevens, 1994: The role of baroclinic processes in tropical cyclone motion: The influence of vertical tilt. *J. Atmos. Sci.,* **51,** 2589–2601.

Franklin, J. L., 1990: Dropwindsonde observations of the environmental flow of Hurricane Josephine (1984): Relationships to vortex motion. *Mon. Wea. Rev.,* **118,** 2732–2744.

——, S. E. Feuer, J. Kaplan, and S. D. Aberson, 1996: Tropical cyclone motion and surrounding flow relationship: Searching for beta gyres in Omega dropwindsonde datasets. *Mon. Wea. Rev.,* **124,** 64–84.

George, J. E., and W. M. Gray, 1976: Tropical cyclone motion and surrounding parameter relationships. *J. Appl. Meteor.,* **15,** 1252–1264.

Gray, W. M., 1975: Tropical cyclone genesis. Dept. of Atmospheric Science Paper 234, Colorado State University, Fort Collins, CO, 121 pp.

Haarsma, R. J., J. F. B. Mitchell, and C. A. Senior, 1993: Tropical disturbances in a GCM. *Climate Dyn.,* **8,** 247–257.

Henderson-Sellers, A., and Coauthors, 1998: Tropical cyclones and global climate change: A post-IPCC assessment. *Bull. Amer. Meteor. Soc.,* **79,** 19–36.

Holland, G. J., 1983: Tropical cyclone motion: Environmental inter-action plus a beta effect. *J. Atmos. Sci.,* **40,** 328–342.

——, Ed., 1993: Tropical cyclone motion. Global Guide to Tropical Cyclone Forecasting, World Meteorological Organization Tech. Document WMO/TD 560, Tropical Cyclone Programme Rep. TCP-31, Geneva, Switzerland. [Available online at http://www.bom.gov.au/bmrc/pubs/tcguide/globa_guide_intro.htm.]

Houghton, J. T., L. G. Meira Filho, B. A. Callander, N. Harris, A. Katenberg, and K. Maskell, Eds., 1996: *Climate Change 1995: The Science of Climate Change.* Cambridge University Press, 572 pp.

——, Y. Ding, D. J. Griggs, M. Noguer, P. J. van der Linden, and D. Xiaosu, Eds., 2001: *Climate Change 2001: The Scientific Basis.* Cambridge University Press, 881 pp.

Jones, S. C., 1995: The evolution of vortices in vertical shear. Part 1: Initially barotropic vortices. *Quart. J. Roy. Meteor. Soc.,* **121,** 821–851.

Knutson, T. R., and R. E. Tuleya, 2001: Impact of CO_2-induced warm-ing on hurricane intensities and simulated in a hurricane model with ocean coupling. *J. Climate,* **14,** 2458–2468.

Li, X., and B. Wang, 1996: Accelerating of hurricane beta drift by shear strain rate of environmental flows. *J. Atmos. Sci.,* **53,** 327–334.

Manabe, S., J. L. Holloway, and H. M. Stone, 1970: Tropical cir-culation on a time-integration of a global model of the atmo-sphere. *J. Atmos. Sci.,* **27,** 580–613.

Shapiro, L. J., 1992: Hurricane vortex motion and evolution in a three-layer model. *J. Atmos. Sci.,* **49,** 140–153.

Vitart, F., and J. L. Anderson, 2001: Sensitivity of Atlantic tropical storm frequency to ENSO and interdecadal variability of SST in an ensemble of AGCM integrations. *J. Climate,* **14,** 533–545.

Walsh, K. J. E., and B. F. Ryan, 2000: Tropical cyclone intensity increase near Australia as a result of climate change. *J. Climate,* **13,** 3029–3036.

Wang, B., and X. Li, 1992: The beta drift of three-dimensional vor-tices: A numerical study. *Mon. Wea. Rev.,* **120,** 579–593.

——, and ——, 1995: Propagation of a tropical cyclone in meridi-onally varying zonal flows: An energetic analysis. *J. Atmos. Sci.,* **52,** 1421–1433.

——, and J.-C. L. Chan, 2002: How strong ENSO events affect tropical storm activity over the western North Pacific. *J. Climate,* **15,** 1643–1658.

——, ——, and L. Wu, 1997: Direction of hurricane beta drift in horizontally sheared flows. *J. Atmos. Sci.,* **54,** 1462–1471.

——, R. Elsberry, Y. Wang, and L. Wu, 1998: Dynamics in the tropical cyclone motion: A review. *Chinese J. Atmos. Sci.,* **22,** 535–547.

Wang, Y., and G. J. Holland, 1996: The beta drift of baroclinic vor-tices. Part II: Diabatic vortices. *J. Atmos. Sci.,* **53,** 3313–3332.

Watterson, I. G., J. L. Evans, and B. F. Ryan, 1995: Seasonal and interannual variability of tropical cyclogenesis: Diagnostics from large-scale fields. *J. Climate,* **8,** 3052–3065.

Williams, R. T., and J. C.-L. Chan, 1994: Numerical studies of the beta effect in tropical cyclone motion. Part II: Zonal mean flow. *J. Atmos. Sci.,* **51,** 1065–1076.

Wu, C.-C., and K. A. Emanuel, 1993: Interaction of a baroclinic vortex with background shear: Application to hurricane move-ment. *J. Atmos. Sci.,* **50,** 62–76.

Wu, G., and N.-C. Lau, 1992: A GCM simulation of the relationship between tropical-storm formation and ENSO. *Mon. Wea. Rev.,* **120,** 958–977.

Wu, L., and B. Wang, 2001: Effects of convective heating on move-ment and vertical coupling of tropical cyclones: A numerical study. *J. Atmos. Sci.,* **58,** 3639–3649.